

A Methodology to Measure Joint Stiffness Parameters for Toolholder-Spindle Interfaces

John S. Agapiou, Manufacturing Systems Research Laboratory, General Motors R&D Center, Warren, Michigan, USA

Abstract

This paper introduces a methodology to evaluate and compare machine tool toolholder-spindle interfaces based on experimental and analytical finite element analysis results. This paper illustrates that the results generated from bench tests (an approach previously used for comparing different sets of interfaces) to characterize toolholder-spindle interfaces do not represent properly the interfaces in a machine tool spindle. The proposed methodology can help standardize the tests and/or the joint parameters required for evaluating, comparing, and selecting toolholder-spindle interfaces by modeling the machine tool spindle itself.

Keywords: Machine Tools, Tooling, Toolholders, Tool Spindles

Introduction

Spindle toolholders are the most critical elements of machining systems, often affecting machining performance because of chatter, part inaccuracy, or spindle failure. The tooling structure is found, in many cases, to be the weakest link in the machining system (Rivin 2000; Shamine and Shin 1999; Stephenson and Agapiou 1997; Weck and Schubert 1994). As the requirements for higher accuracy, higher speeds, and higher power in machining increase, it becomes increasingly important to understand the interaction of the toolholder interface with the spindle and the cutting tool to minimize deflection and modal instability.

There are several issues to consider, including joint stiffness, accuracy, and so on, when selecting the proper toolholder interface for a given range of applications. Information currently exists on the static, dynamic, and accuracy characteristics of several interfaces, as measured by different institutions using similar or different test setups and/or methods (Hanna, Agapiou, and Stephenson 2002; Hazem et al. 1987; Jacobs 1999; Tsutsumi 1985; Weck and

Schubert 1994); such data are based on tests performed on a spindle system specifically designed to accentuate the characteristics of the joint between the spindle and the toolholder. Using these data, an engineer makes a suitable selection of a toolholder-spindle interface for a specific range of applications in a machining system. A systematic universal approach is needed for evaluating and selecting toolholder interfaces.

Limited finite element analysis (FEA) has been used to examine static and dynamic performance of the interface, including the effects of varying toolholder and spindle taper geometry, clamping load, spindle speed, applied bending load, and applied rotational load (Aoyama and Inasaki 2001; Hanna, Agapiou, and Stephenson 2002; Kim, Wu, and Eman 1989; Shamine and Shin 1999; Tsutsumi 1995; Wang and Horng 1994; Weck and Schubert 1994; Wyatt Becker et al. 1999). Generally, only the toolholder and the interface are modeled, while the finite element model (FEM) of the main spindle generating the cutting movement is neglected due to complexity and size of the model. The joint dynamic parameters are very important but difficult to model or estimate accurately due to the inability to measure the response at the interface, which is inaccessible (Kim, Wu, and Eman 1989; Wang and Horng 1994; Shamine and Shin 1999).

This paper demonstrates that a toolholder-spindle interface should be evaluated in a machine spindle and not in a bench fixture. It also explains the requirement of using the joint stiffness parameters for evaluating or comparing toolholder interfaces when not using a physical spindle. In addition, a methodology is developed to experimentally determine the toolholder-spindle interface characteristic joint stiffness parameters using 2-D finite element modeling.

A 2-DOF (degrees of freedom) spring with linear and rotational stiffness components is extracted from

This paper is an original work and has not been previously published except in the *Transactions of NAMRI/SME*, Vol. 32, 2004.

a 2-D FEM of the bench test fixture and is evaluated against two other approaches based on: (1) the FEA in ABAQUS finite element code and (2) a method based on rigid-body dynamics and frequency response function (FRF) measurements. The joint parameters of a particular interface can be used in modeling spindle system dynamics. The procedure has been executed with good results for stiffness determination. This method can be refined and adapted universally for generating common data for all available interfaces. Such data can be used during the design of spindle interfaces, for selection of proper cutting conditions in a target application, or for comparing toolholder interface styles.

Evaluation of Interface

The objective of this paper is to identify a common procedure for evaluating toolholder-spindle interfaces. The evaluation considers two basic styles of toolholder-spindle connections: (1) conventional steep-taper CAT-40 style and (2) hollow-shank HSK-A63 style.

Experimental Setup and Measurement Procedure

A special setup (illustrated in *Figure 1*) was designed to isolate the toolholder interface. The steel table test stand consisted of a very stiff spindle made of a cast iron block (with dimensions of 305 mm × 356 mm × 406 mm and mass $m = 327$ kg), a spindle nose (140 mm diameter × 100 mm long on a 51 mm flange attached to the block using eight 0.75-10 bolts on a 222 mm bolt circle), and a test tool (44.45 mm diameter × 100 mm long). The steel spindle noses were designed to represent the ends of machine tool spindles, with various connections for the toolholder. The simulated tools were intentionally made large to accentuate the characteristics of the connection. An instrumented drawbar was used to pull the tool into the spindle nose at specified clamping pre-loads. The CAT-40 and HSK-A63 test tools were made monolithic. The taper shanks were the only difference among them.

The static test involved measuring a deflection at the end of the tool with a capacitance gage. During the static deflection testing, the block was clamped on a steel table. The static stiffness was evaluated at a force of 2,000 N (applied to the end of the tool), while high-load static testing was required for mea-

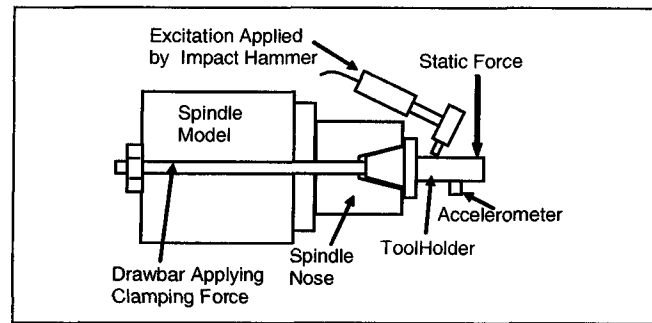


Figure 1
Experimental Test Setup for Measuring Toolholder Characteristics

suring the tipping angle and estimating the angular or normalized bending stiffness (Jacobs 1999).

The modal testing theory has been successfully used for calculating the frequency spectrum of machine tool structures (Ewins 1984). The dynamic test provides a means to measure the FRF of the toolholder interface system (Jacobs 1999). During the dynamic testing, the block was placed on a rubber isolation mat to represent the free-free vibration of the test setup.

Finite Element Modeling of Bench Fixture

Three different methods were evaluated for estimating the joint stiffness parameters of an interface using more than just a linear spring as in the previous research work (Kim, Wu, and Eman 1989; Shamine and Shin 1999; Wang and Horng 1994). In the first method, the SPA spindle analysis program from Manufacturing Laboratories, Inc. was used to create a two-dimensional axisymmetric model that matched the geometry of the test block, spindle nose, and test tool. SPA is a fast, special-purpose software to analyze machine tool spindles and their tooling. The program can model a 2-DOF spring to include a linear direction and rotational direction, as illustrated in *Figure 2a*. Hence, a spring with linear and rotational components to represent a joint between the spindle and the toolholder is illustrated as spring S3 in *Figure 2b*. The SPA FEA program is traditionally capable of simulating both the dynamic and static behavior of a spindle and tooling system. In the past, two linear springs (one at each end of the taper interface (as illustrated in *Figure 3*) have been utilized to model the CAT taper joint (Kim, Wu, and Eman 1989; Wang and Horng 1994; Shamine and Shin 1999). However, the use of two parallel linear springs (with equivalent stiffness of the sum of the individual spring stiffnesses) seems to be somewhat insufficient

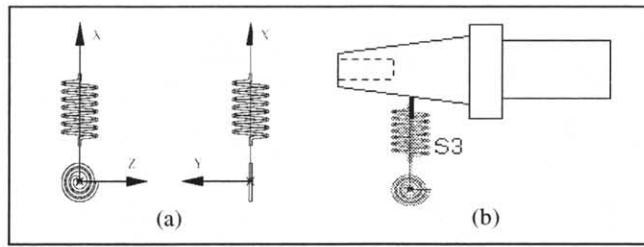


Figure 2
2-DOF (linear and rotational) Spring Orientations Used in SPA FEA Model

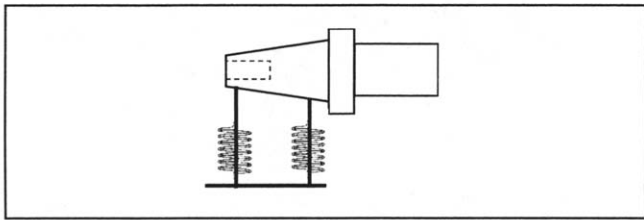


Figure 3
FEA Model Using Two Linear Springs

to universally represent the joint parameters of an interface based on the inconsistency among the published results of the CAT interfaces (Kim, Wu, and Eman 1989; Wang and Horng 1994; Shamane and Shin 1999).

The bench test setup (as illustrated in *Figure 4*) consisted of two parts, the test block and the spindle nose as one piece and the toolholder as the second piece. The tapered area of the spindle nose and toolholder interface was modeled by dividing the length of the taper into four equally spaced elements.

To simulate the bench fixture in the FEA model, both the linear and rotational spring constants for the connection of the block to ground (S1 and S2 in *Figure 4*) were set to be soft, approximately 7.6×10^8 N/m and 7.6×10^9 Nm/rad, respectively. The joint between the toolholder and the spindle nose is represented by spring S3. The parameters of spring S3 were determined by matching the measured dynamic response and static deflections to those generated by the FEM analysis. This involved adjusting the location of the nodes that defined the joint along with the linear and rotational spring constants associated with spring S3. This resulted in the joint location and the spring constants associated with the connection.

Although many combinations of bending and rotational stiffness will correctly predict the static deflection at the tip of the tool, the matched model was also required to predict the natural frequencies and modal stiffness.

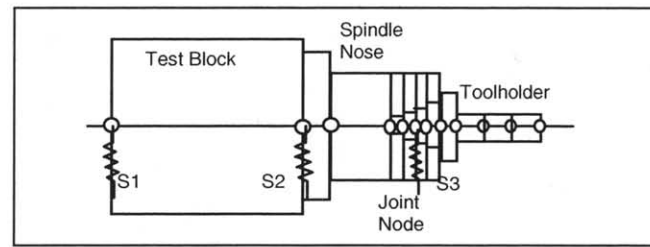


Figure 4
SPA FEA Model for the Setup

The second method for estimating the joint stiffness parameters was evaluated using ABAQUS/Standard finite element code. The ABAQUS/Standard was used to model the bench fixture assembly with appropriate contact interactions between components using a full 3-D model. The effective joint stiffness, k , at a given load P , is defined as the angular stiffness

$$k = \frac{P \cdot L}{\theta} = \frac{P \cdot L^2}{\delta - \delta_f} \quad (1)$$

where L is the distance from the point of load application to the top of the spindle surface, δ is the deflection predicted from the FEA, and δ_f is the deflection of the toolholder when it is rigidly connected to ground at its taper shank. The deflection was calculated by applying 2,000 N lateral load in the model. If the toolholder joint were to be replaced by a rotational spring with the stiffness given by Eq. (1), the deflection under a lateral load would be the same as the deflection obtained with the full assembly model.

Rigid-Body Dynamics to Measure Joint Parameters

The third method for estimating the joint stiffness parameters was based on rigid-body dynamics and FRF measurements, and which was also evaluated for the determination of joint stiffness (Wyatt Becker et al. 1999). This method provides a 6×6 stiffness matrix for the joint by simultaneously determining the stiffness components in six coordinate directions (three translations, three rotations), including the pivot point location. This method circumvents the limitations associated with joint stiffness testing of single-direction measurements. Wyatt Becker et al. explain the mathematical formulation in the reference.

The test structure consists of two cylinders that are connected through an interface in a way similar

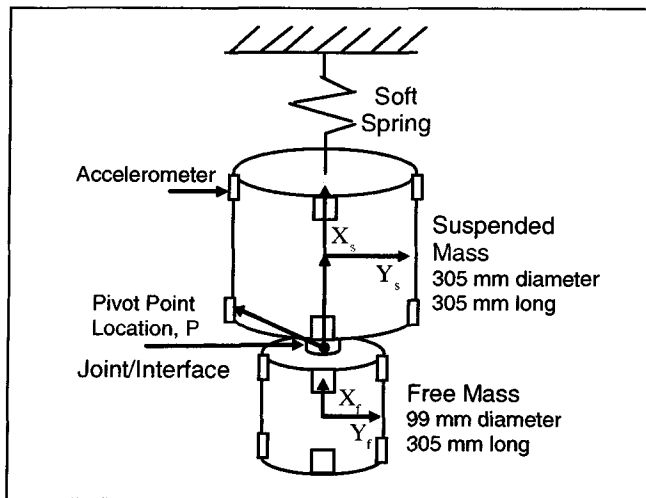


Figure 5
Diagram of Test Setup Used in Rigid-Body Dynamic Method

to the actual identical connections in machining (see *Figure 5*). The testing fixture was suspended on a soft support to simulate free-free boundary conditions and was excited by impacting on the larger mass, the suspended one.

Once the stiffness values have been calculated, the measured frequency and damping values are the results of parameter estimation performed on the recorded FRF data. The pivot point is selected by matching the estimated frequencies of bending to the measured values.

Experimental and Analytical Results

The experimental bench test results and analytical/modeling results on joint stiffness parameters were evaluated by comparing the CAT-40 interface with the HSK-A63 interface.

Experimental Results

Static and dynamic bending stiffness were measured from the bench fixture tests using three clamping levels for the CAT-40 (7, 12, 17 kN) and four levels for the HSK-A63 (10, 14, 18, 24 kN). A photo of the experimental bench test setup is shown in *Figure 6*. A comparison of the bending stiffness of the two interfaces is given in *Figure 7*. The static bending stiffness for the HSK-A63 interface is about 60-70% greater than that of the CAT-40 interface. The static and modal stiffness saturates at the lower draw-bar pre-loads (7 kN and 10 kN, respectively, for the CAT-40 and HSK-A63 interfaces).

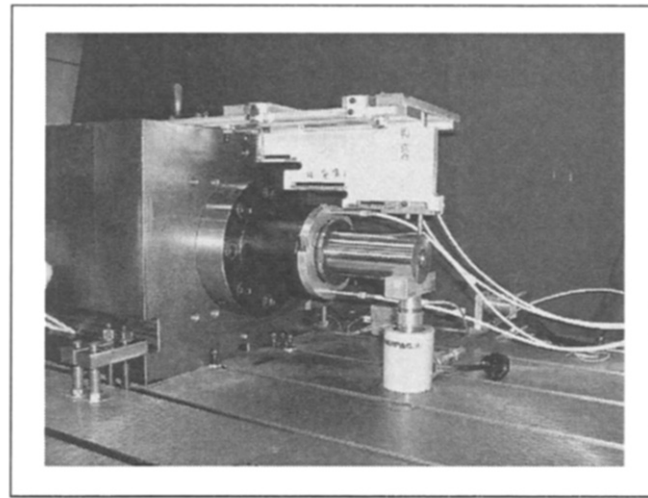


Figure 6
Experimental Bench Test of Toolholder (CAT-40 is shown)

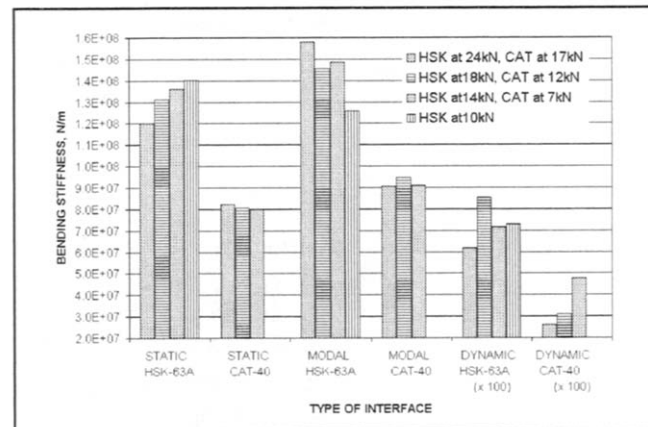


Figure 7
Static, Modal, and Dynamic Bending Stiffness of Toolholder Interfaces for Various Clamping Forces

The dynamic bending stiffness (defined as the product of modal stiffness with damping ratio) for the HSK-A63 interface is also much better than for the CAT-40 (see *Figure 7*). In addition, the modal stiffness decreases while the dynamic stiffness increases with a decrease in the clamping force for both styles of interfaces.

The measurement of the toolholder tilting at the interface under an applied bending moment provides a normalized measurement of static bending stiffness (Jacobs 1999) among the two interfaces, and it is given in *Figure 8*. The HSK-A63 provides about 200-300% higher stiffness than the CAT-40 interface at bending moments lower than 200 Nm. The normalized bending stiffness is reduced with increasing bending moment for the HSK interface. The nor-

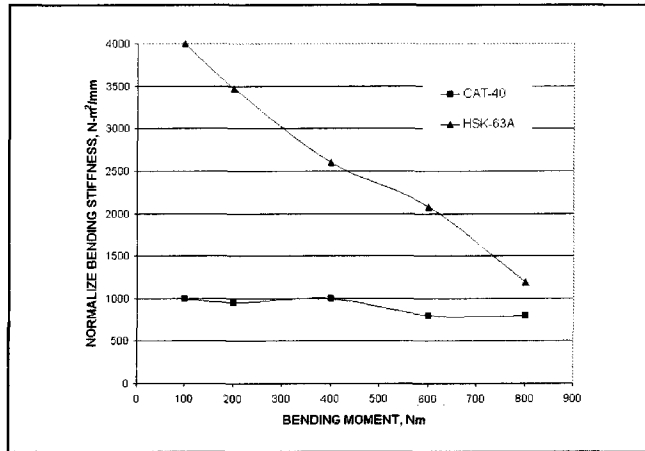


Figure 8
Normalized Static Bending Stiffness for HSK-A63 and CAT-40 Interfaces

malized stiffness was found to be the same for all the clamping forces for bending moments less than 200 Nm. The boundary bending moment for an HSK-A63 is much greater than that of a CAT-40. The bench test results of the static and dynamic stiffness indicate that the HSK-A63 interface is superior to CAT-40 interface.

Joint Stiffness Parameters Identification

The effective joint parameters were determined by matching the measured dynamic response and static deflections to those generated by the FEA based on the SPA model (see Figure 4) of the bench fixture. The estimated average joint location and the linear and rotational spring constants (see Figure 3) associated with the interfaces are given in Table 1.

Tables 2 and 3 compare the measured dynamic response and static deflections to those calculated by the FEA. From Table 2, it can be seen that the estimated natural frequency and modal stiffness for the first significant mode of vibration show good agreement with measured results. For the second and third modes of vibration, the measured and calculated natural frequencies varied less than 13%, while the modal stiffness varied approximately 30-90%. This level of correlation was typical of the HSK-A63 interface. It can be seen from Tables 2 and 3 that the FEA model using the joint parameters in Table 1 provides a reasonable prediction of the modal parameters and static stiffness of the total system.

The rotational spring joint stiffness estimated by the 3-D FEM in ABAQUS is 8.34×10^5 Nm/rad and

Table 1
Average Joint Characteristics for the CAT-40 and HSK-A63 Interfaces

Interface	Joint Location (m)	Spring Constants	
		Linear (N/m)	Rotational (Nm/rad)
CAT-40	0.02	1.375E+09	8.108E+06
HSK-A63	0.02	2.335E+09	1.587E+07

Table 2
Comparison Between Measured (FRF Test) and Calculated Modal (FEA) Parameters for the CAT-40 Interface (at 17 kN clamping force)

Measured Modal Bending Parameters				
Mode	ω_n (Hz)	K (N/m)	Mass (kg)	ζ
1st	2124	9.21E+07	0.5169	0.0025
2nd	3205	8.52E+08	2.2369	0.0076
3rd	3937	8.14E+09	13.3090	0.0027
FEA Model Modal Bending Parameters				
1st	2125	1.19E+08	0.6675	0.0025
2nd	3645	5.70E+08	1.0860	0.0025
3rd	4065	9.09E+08	1.3931	0.0025

Table 3
Comparison Between Measured and Calculated (FEA) Static Stiffness for the CAT-40 Interface (at 17 kN clamping force)

Applied Load (N)	Measured K (N/m)	Calculated (FEA) K (N/m)
2000	9.417E+07	8.696E+07

Table 4
Estimated Joint Parameters from Rigid-Body Dynamics Method

	CAT-40	HSK-A63
Joint location (m)	0.061	0.063
Rotation (Nm/rad)	7.300E+05	1.788E+06
Rotational 1 (Nm/rad)	2.006E+06	4.309E+06
Rotational 2 (Nm/rad)	1.865E+06	4.399E+06

9.9×10^5 Nm/rad, respectively, in the directions along and perpendicular to the keys for CAT-40.

The results for the rigid-body dynamics method are given in Table 4. It was found that the translation stiffness components could not be extracted from the stiffness matrix using the fixture size in Figure 5. The joint parameters results from the bench test illustrate that the HSK-A63 is superior to CAT-40.

In an effort to compare the results from the three approaches, an effective bending (rotational) spring was estimated to be 5.93×10^6 Nm/rad using Eq. (1), and the deflections from Table 5 were used for the proposed methodology.

Replacing the spring S3 in the SPA FEA model with a spring having a very stiff linear component ($1E+19$ N/m) and with the rotational component to

Table 5
Spring Constants and Resulting Deflections for CAT-40 Interface from the Proposed Method (Figure 3)

Spring S3		Deflection (mm)	
Linear (N/m)	Rotational (Nm/rad)	\ddot{a}	\ddot{a}_f
1.375E+09	8.108E+06	0.0230	
1.000E+19	1.000E+19		0.0177

Table 6
Comparison of Static and Dynamic Parameters Predicted from SPA FEA as a Result of Varying the Spring Constants Associated with Spring S3 for CAT-40 Interface

Spring S3		Calculated Modal		Static
Linear (N/m)	Rotational (Nm/rad)	ω_n (Hz)	K (N/m)	Deflection (mm)
1.38E+9	8.108E+6	2120	1.20	0.0230
		3644	5.50	
		4055	9.17	
1.0E+19	5.93E+6	2367	9.75	0.0230
		3716	3.00	
		5133	1.78	

be 5.93×10^6 Nm/rad as calculated above results in an equivalent deflection at the tip of the tool as shown in Table 6.

This indicates that there are at least two combinations of spring constants for spring S3 that will result in the desired static deflection but may not accurately describe the dynamics of the system, as illustrated in Table 6. Therefore, spring S3 with linear and rotational components, as proposed in this paper, better represents the toolholder-spindle interface than a single linear or rotational spring. The use of only one spring constant was insufficient to properly represent the joint parameters of an interface.

Validation of Methodology

Analysis of Machine Tool Spindle

The SPA FEA program was used to construct a model of the spindle for the machine tools available in our lab for evaluating the CAT-40 and HSK-A63 interfaces while validating the methodology for characterizing the toolholder-spindle interface. The spindle shaft and the housing were modeled as illustrated in Figure 9.

The taper joint stiffness parameters, obtained from the previous two steps of the methodology, are used here to model the interface with the 2-DOF spring S3 (explained in Figure 2). Springs S1, S2, and S4 represent the spindle bearings, and springs S5 and

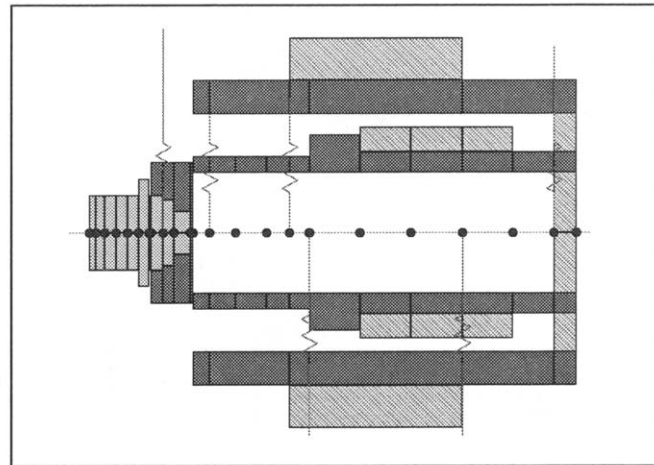


Figure 9
SPA Model for CAT-40 Spindle

S6 represent the connection of the spindle housing to the machine tool structure. The toolholder structure used in the bench test was modeled here. Both toolholder styles, CAT-40 and HSK-A63, were tested in two identical machines with identical spindles but different interface styles.

Results from SPA for Spindle Systems

The CAT-40 and HSK-A63 interfaces were modeled in the spindle given in Figure 9. The joint parameters estimated in Table 1 were used in the SPA model to represent spring S3. The static and modal analysis results are given in Tables 7 and 8, respectively. The toolholder deflection and natural frequencies or mode shapes were similar for both interface styles.

Experiment Results from Machine Tool Spindle

Comparison of the static bending stiffness between the HSK and CAT interfaces in identical machine tool spindles is shown in Figure 10. The tool stiffness is about equal for both interfaces especially below 600 N radial force at the tool end. On the contrary, the results from the bench tests are also shown in Figure 10, and these illustrate that the HSK interface is much stiffer than the CAT system (as explained in Figures 7 and 8).

The natural frequencies for the two interfaces from the machine tool spindle tests were in good agreement, with a difference of less than 5%. The modal stiffness for the CAT-40 was somewhat larger than that of the HSK-A63. The first two natural frequencies from the SPA FEA (in Table 8) were within 5% those from the machine tool spindles. In addition,

Table 7
Comparison of Estimated Static Stiffness (from SPA)
in the Machine Spindle

Applied Load (N)	CAT-40 (N/m)	HSK-A63 (N/m)
1000	2.622E+07	2.706E+07

Table 8
Comparison of Estimated Modal Parameters (from SPA)
in the Machine Spindle

Mode	CAT-40		HSK-A63	
	ω_n (Hz)	K (N/m)	ω_n (Hz)	K (N/m)
1st	517	1.39E+08	517	1.45E+08
2nd	671	4.10E+07	675	4.22E+07
3rd	1521	3.12E+08	1532	3.33E+08

the natural frequencies are much lower when the toolholder is in the spindle than when it is in the bench fixture (compare *Tables 8* and *2*). These results emphasize the importance of evaluating the toolholder system on the actual production spindle instead of on a bench test.

Summary and Conclusions

The above work resulted in a methodology for estimating joint stiffness parameters for a toolholder-spindle interface. The flow chart of the methodology is given in *Figure 11* and was validated using the CAT-40 and HSK-A63 interfaces.

The methodology in *Figure 11* for evaluating and comparing the toolholder-spindle interfaces was developed. The paper also explains why it is important to establish standardized joint stiffness parameters for evaluating or comparing toolholder interfaces in a machine tool spindle and not just on a bench fixture as has been the case in the past.

This analysis demonstrates the importance and benefits of the static and dynamic stiffnesses. It illustrates the significant difference between results extracted from bench fixture tests and machine tool spindle tests of identical interfaces. It illustrates that the static and dynamic stiffnesses seen at the tip of the cutting tool also depend on the stiffnesses of the tool, the spindle geometry and bearings, the housing, and the overall machine structure. The methodology in this paper provides the opportunity to evaluate several styles of toolholder interfaces in a spindle without performing actual tests on the spindle.

The 2-DOF spring concept utilized in the model has an advantage over the linear spring (used by other researchers) for calculating the static and dy-

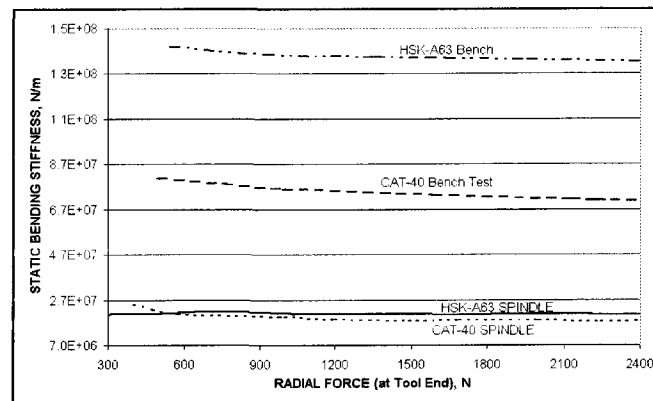


Figure 10
Comparison of Static Bending Stiffness Between CAT-40 and HSK-A63 Toolholders on Bench Fixture and in Machine Tool Spindle

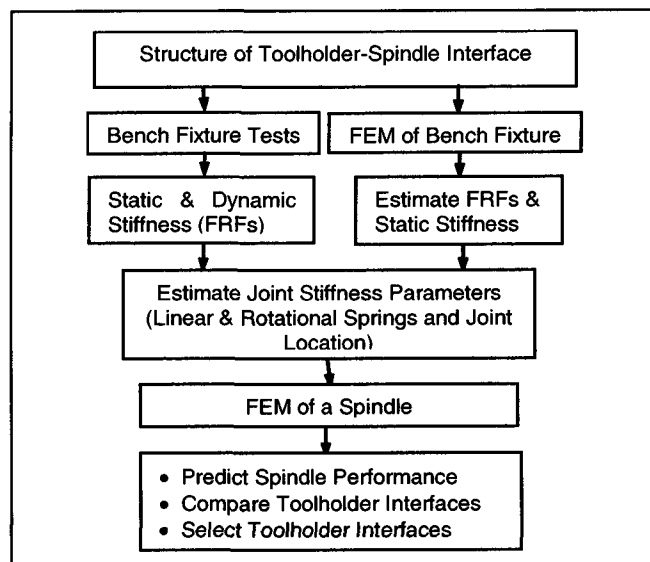


Figure 11
Flow Chart of Methodology for Evaluating Interfaces

namc toolholder-joint-spindle system bending stiffnesses and mode shapes.

The static and dynamic performance of the CAT-40 interface can be similar to that of the HSK-A63 interface in a machine tool spindle compared to the CAT-40's inferior performance obtained from bench tests in a fixture.

Acknowledgments

The author extends appreciation to S. Smith and P. Jacobs at the University of North Carolina-Charlotte and W.H. Robert at the University of Cincinnati for their collaboration in evaluating several of the toolholder-spindle interfaces. The author also would like to thank the following toolholder com-

panies—Command, Parlec, Briney, Lyndex, and Kennametal—for supporting the experimental work with UNCC and UC and their suggestions throughout the project. Additional thanks are extended to B. Haukkala, D. Stauffer, J. McCabe, C.H. Shen, D. Stephenson, M. Gillman, and P. Bandyopadhyay for their support and suggestions throughout the completion of this project.

References

- Aoyama, T. and Inasaki, I. (2001). "Performances of HSK tool interfaces under high rotational speed." *Annals of the CIRP* (v50, n1), pp281-284.
- Ewins, D.J. (1984). *Theory and Practice in Modal Testing*. New York: John Wiley & Sons, Inc.
- Hanna, H.; Agapiou, J.S.; and Stephenson, D.A. (2002). "Modeling the HSK toolholder-spindle interface." *Trans. of ASME, Journal of Mfg. Science and Engg.* (v124, n3), pp734-744.
- Hazem, S.; Mori, J.; Tsutsumi, M.; and Ito, Y. (1987). "A new modular tooling system of curvic coupling type." *Proc. of 26th Int'l Machine Tool Design and Research Conf.* MacMillan, pp261-267.
- Jacobs, P.T. (1999). "Characterization of the machine tool spindle to toolholder connection." Master's thesis. Univ. of North Carolina at Charlotte.
- Kim, T.R.; Wu, S.M.; Eman, K.F. (1989). "Identification of joint parameters for a taper joint." *Trans. of ASME, Journal of Engg. for Industry* (v111), pp282-287.
- Rivin, E.I. (2000). "Tooling structure: interface between cutting edge and machine tool." *Annals of the CIRP* (v49, n2), pp591-634.
- Shamine, D.M. and Shin Y.C. (1999). "Analysis of No. 50 taper joint stiffness under axial and radial loading." *Transactions of NAMRI/SME* (v27). Dearborn, MI: Society of Manufacturing Engineers, pp111-116.
- Stephenson, D.A. and Agapiou, J. (1997). *Metal Cutting Theory and Practice*. New York: Marcel Dekker Inc., pp286-406.
- Tsutsumi, M.; Nakai, K.; and Anno, Y. (1985). "Study of stiffness of tapered spindle connections." *Trans. of the Japan Society of Mechanical Engineers* (vC51), pp1629-1637.
- Tsutsumi, M.; Kuwada, T.; et al. (1995). "Static and dynamic stiffness of 1/10 tapered joints for automatic changing." *Int'l Journal of the Japan Society for Precision Engg.* (v29, n4), pp301-306.
- Wang, J.H. and Horng, S.B. (1994). "Investigation of the tool holder system with a taper angle 7:24." *Int'l Journal of Machine Tools and Manufacture* (v34, n8), pp1163-1176.
- Weck, M. and Schubert, I. (1994). "New interface machine/tool: hollow shank." *Annals of the CIRP* (v43), pp345-348.
- Wyatt Becker, P.J.; Wynn Jr., R.H.; Berger, E.J.; and Blough, J.R. (1999). "Using rigid-body dynamics to measure joint stiffness." *Mechanical Systems and Signal Processing* (v13, n5), pp789-801.

Author's Biography

John Agapiou received his PhD from the University of Wisconsin-Madison in 1985. He is currently a staff research engineer in the Manufacturing Systems Research Lab at the General Motors R&D Center (Warren, MI). His research interests are optimization of metalcutting operations, including the cutting tool and toolholders, agile/flexible manufacturing, modeling metalcutting operations, modeling manufacturing quality for machining lines, and high-speed machining.